

A SIMPLIFIED LARGE-SIGNAL HBT MODEL FOR RF CIRCUIT DESIGN

Ke Lu, Xiangdong Zhang, Gregory N. Henderson

Corporate R&D Center, AMP M/A-COM Inc

100 Chelmsford St. Lowell, MA 01853-3294, USA.

Abstract: A simplified version of UCD HBT model[6] has been presented in this paper. Two nonlinear resistors in UCD model are replaced by the linear resistors. Three new nodes are added to the model which allows one to model the thermal interaction between emitter fingers in a multi-cell power HBT. A scaling factor is also included. All model parameters can be extracted by a group of standard DC and small-signal S-parameters measurements. Large-signal measurement results, such as power-sweep and intermodulation at several different bias points are used to verify the new model. The agreement between simulated and measured results is excellent.

I. Introduction:

AlGaAs/GaAs HBTs have been widely accepted in many RF/Microwave applications including power amplifiers, oscillators and mixers. An accurate large-signal HBT model plays a fundamental role in designing these circuits [1-6]. The model developed by Lu, Perry, Brazil in University College Dublin (UCD) is an unique HBT model which has a different topology than the conventional Ebers-Moll or Gummel-Poon model [6]. The UCD model also possesses other novel features such as: the capability of modeling self-heating, collector-transit time, non-uniform current gain, and direct model parameter extraction strategy. In this paper, a simplified UCD model is introduced to model the M/A-COM 16-finger baseline HBT. The new model significantly reduces the number of nonlinear circuit elements in the UCD model without compromising accuracy. A scaling factor is also included in the present model to make model scalable.

II. New HBT Model:

The new intrinsic large-signal HBT model is shown in Figure 1(a) and (b). It uses two temperature-dependent diodes D_{BE_IB} and D_{BE_IC} to describe the base and collector currents in the forward-bias region. The I-V relationships for these two diodes are given by:

$$I = A_E \cdot I_{S_IB}(T_J) \cdot \left(\exp\left(\frac{V}{n_{BE_IB}(T_J) \cdot V_T}\right) - 1 \right)$$

for D_{BE_IB} (1)

$$I = A_E \cdot I_{S_IC}(T_J) \cdot \left(\exp\left(\frac{V}{n_{BE_IC}(T_J) \cdot V_T}\right) - 1 \right)$$

for D_{BE_IC} (2)

where V and I are the voltage and current applied to the diode ports, n_{BE_IB} and n_{BE_IC} are the temperature-dependent ideality factor of two diodes, A_E is the scaling factor. Temperature-dependence in the diode characteristics is introduced by the temperature-dependent ideality factor and saturation current [1]:

$$I_S(T_J) = I_S(T_0) \cdot \exp\left(T_S \cdot \left(\frac{1}{T_0} - \frac{1}{T_J}\right)\right) \quad (3)$$

$$n(T_J) = n(T_0) \cdot \left(1 + A_n \cdot \Delta T + B_n \cdot \Delta T^2\right) \quad (4)$$

where T_0 is the ambient temperature, T_S , A_n , B_n are the model parameters. Equations (1-4) represent a major difference in modeling base and collector currents as compared to the classic Ebers-Moll or Gummel-Poon model. In the new model, the base and collector currents are directly controlled by the electrical potential across the base-emitter junction. The direct relationship between base and collector currents (via current gain β_F) in the EM or GP model is replaced by an indirect relationship (via V_{BE} and base contact resistances). This particular setup is a major departure of the new model from the conventional GP and EM model. In the previous UCD model, two nonlinear base resistances are used to track the base and collector current in the high-current region. In the present model, two constant base resistors R_{BI_IB} and R_{BI_IC} are used to replace these two nonlinear base resistances without introducing big errors in the high-current region. The new model not only predicts correct DC current gain but also the derivatives of DC current gain. This novel features enables the model to accurately predict intermodulation components. The junction temperature is calculated from the dissipated power inside the HBT by

$$P_D = V_{BE} \cdot I_B + V_{CE} \cdot I_C \quad (5)$$

$$T_J(t) = \int_0^t Z_{TH}(t-t') \cdot P_D(t') \cdot dt' + T_A \quad (6)$$

$$\text{or } T_J(\omega) - T_A = Z_{TH}(\omega) \cdot P_D(\omega) \quad (7)$$

where V and I are the instantaneous port voltage and current. Junction temperature is calculated based on the instantaneous dissipated power, thermal resistance and thermal capacitance [8]. The temperature effect is implemented in a novel way (three extra thermal nodes are added into the new model) so that the users can easily insert the model to a thermal equivalent circuit which may be coupled with other devices in the same die. Meanwhile, multi-finger power HBTs can also be modeled by a group of single intrinsic HBTs coupled by a thermal network [5,7], Figure 1(c). The model also has been used to simulate current gain collapse or current hogging in the multi-finger HBTs [7]. The temperature-effect is implemented in a true time-domain fashion and the junction temperature can be predicted at both DC and RF situations. It is worth indicating that equation (5) is not only a low-frequency approximation, but it is applicable to RF frequencies. The diode D_{BC} is used to model the collector current in the reverse bias condition. There are two nonlinear capacitances $C_{BE}(V_{BE}, V_{BC})$ and $C_{BC}(V_{BC})$ in the present model. In the forward region, the charge components (which is obtained by path integration of $C_{BE}(V_{BE}, V_{BC})$) of associated with V_{BE} can be modeled by

$$Q_{DE} = \tau_F \cdot I_{CC} \quad (8)$$

$$\tau_F = \tau_0 + \tau_B \cdot \left(1 - \frac{V_{BC}}{\phi_{BC}}\right)^{M_{JBC}} \quad (9)$$

where τ_F is the total transit time for an electron to pass the emitter, base and base-emitter depletion region. τ_0 is the transit time for electrons to reach the boundary of BC SCR and it is not bias-dependent. The second term in (9) is used to model the transit time for an electron to pass the BC SCR which is V_{BC} dependent. The $C_{BE}(V_{BE}, V_{BC})$ is obtained by differentiating (8) with respect to V_{BE} .

III. Parameter Extraction Procedure

The usefulness of a large-signal model for a circuit designer is fully dependent on the how accurate the model parameters can be extracted. The new model yields a very simple parameter extraction procedure. Most of the model parameters can be extracted by

direct DC and AC measurement results. The parameters in (1-4) can be extracted by performing Gummel-plot measurements at a few different ambient temperatures. The emitter resistance can be extracted by the open-collector method. Two base resistances are estimated by the Gummel-plot results in high current region. The thermal resistance can be estimated from the IV data. The nonlinear $C_{BE}(V_{BE}, V_{BC})$, and $C_{BC}(V_{BC})$ are extracted from multi- S-parameter measurement results.

IV. Verification of New Model

After all the model parameters are available, the model is ready to be verified. Since the model parameters are extracted from DC and small-signal AC results, the large-signal power measurements can be considered as an independent verification method. The model predicts accurate DC gain (Figure 2), its derivatives (Figure 3) and small-signal S parameters. The bias-dependence of the C_{BE} and C_{BC} are accurately modeled by (8) and (9), as shown in Figure 4. Figure 5 shows the comparison between measured and simulated power-sweep results under constant V_{BE} . The bias point shifting can also be predicted by the new model, as shown in Figure 6. Figure 7 and 8 show the power-sweep results at a constant I_B bias condition. Since the new model is able not only predict the correct DC gain, but also the differential gain (Figure 3), it is an accurate tool to predict the linearity performance of HBTs, as shown in Figure 9 and 10. The new model can be scaled up and down with a one scaling factor A_e . The new model has also been used for the design of HBT MMIC amplifiers.

V. Conclusions

A simple large-signal model is presented in this paper. The model includes the most important behaviour of AlGaAs/GaAs HBTs such as the self-heating effect, nonuniform current gain, thermal-coupling among the emitter fingers, and BC SCR width modulation. The agreement between simulated and measured large-signal power-sweep and IM3 results are excellent.

Acknowledgments:

The authors would like to thank our HBT teams: A. Hanson, M. Fukuda, C. McLean, Y. Yun, J. Atherton, M. O'Keefe, P. Ersland, J. Chi for their help. The encouragement and support from Dr. Peter Staeker is greatly appreciated.

References:

- [1] P. C. Grossman, J. Choma, Jr, "Large signal modeling of HBT's including self-heating and transit time effects," IEEE Trans. Microwave Theory and Tech., Vol. 40, pp. 449-464, March 1992

- [2] C. Wei, J. C. M. Hwang, W. Ho, J. A. Higgins, "Large-signal modeling of self-heating, collector transit-time, and RF-breakdown effects in power HBTs", IEEE Trans. Microwave Theory and Tech., Vol. 44, pp. 2641-2647, Dec. 1996
- [3] A. Samelis, D. Pavlidis, "Analysis of the large-signal characteristics of power heterojunction bipolar transistors exhibiting self-heating effects", IEEE Trans. Microwave Theory and Tech., Vol. 45, pp.534-542, April 1997
- [4] D. Wu, M. Fukuda, Y. Yun, "A novel extraction method for accurate determination of HBT large-signal model parameters," IEEE MTT-S Digest pp.1235-1238, 1995
- [5] C. M. Snowden, "Large-signal microwave characterization of AlGaAs/GaAs HBT's based on a physics-based electrothermal model", IEEE Trans. on Microwave Theory and Techniques, Vol.45, pp.58-71, January 1997
- [6] Ke Lu, P. A. Perry, T. J. Brazil, "A new large-signal AlGaAs/GaAs HBT model including self-heating effects, with corresponding parameter-extraction procedure," IEEE Trans. on Microwave Theory and Techniques, Vol.43, pp.1433-1445, July 1995
- [7] Ke Lu, C. M. Snowden, "Analysis of thermal instability in multi-finger power AlGaAs/GaAs HBT's", IEEE Trans. on Electron Devices, Vol.43, No.11, pp.1799-1805, 1996
- [8] K. Lu, X. Zhang, "Characterization and modeling of thermal dynamic behavior of AlGaAs/GaAS HBTs", 1998 IEEE MTT-S Digest, 1998

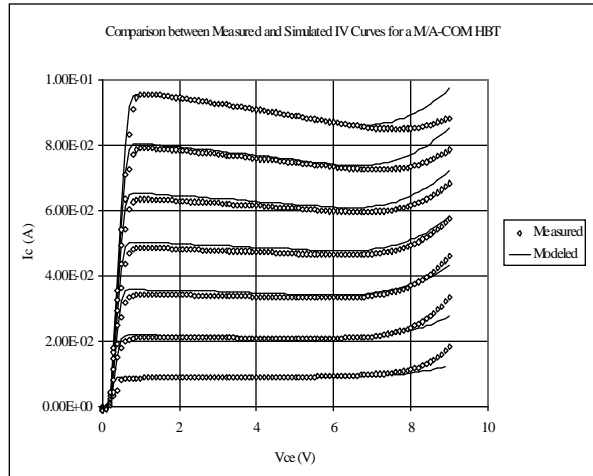


Fig.2 Comparison between modeled and measured HBT output IV characteristics

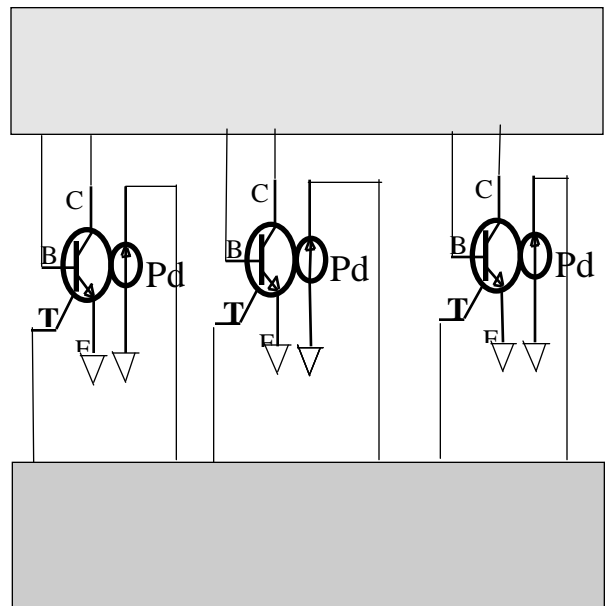
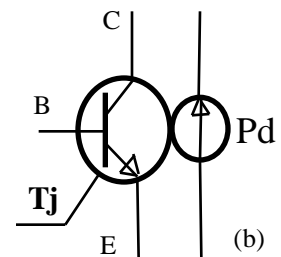
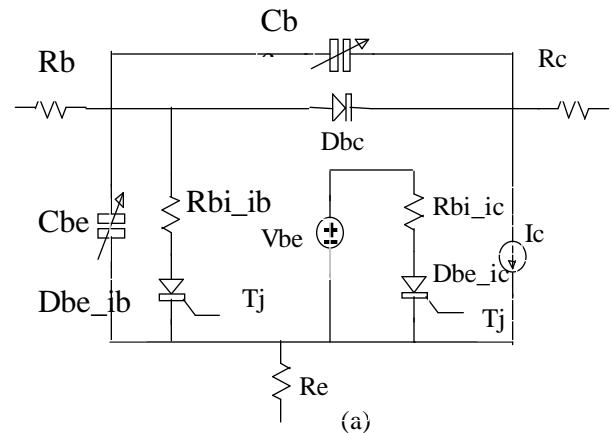


Fig.1 Large-signal HBT model with self-heating.
 (a) Intrinsic device model; (b) Model symbol; (c)
 Modeling several HBT in a thermo-electrical
 interactive environment.

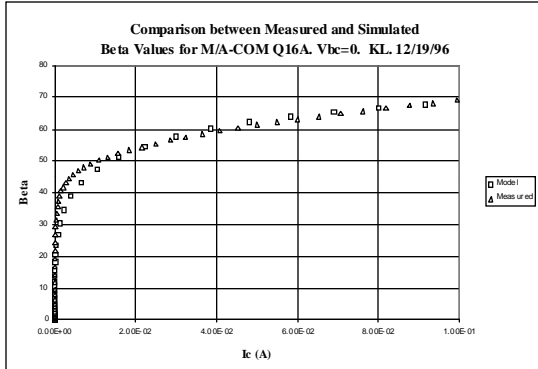


Fig.3 Measured and simulated differential gain.

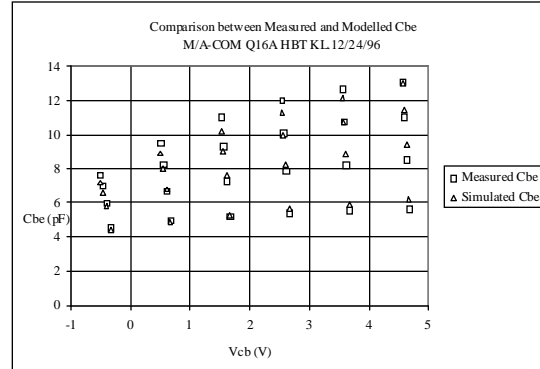


Fig.4 Measured and simulated Cbe.

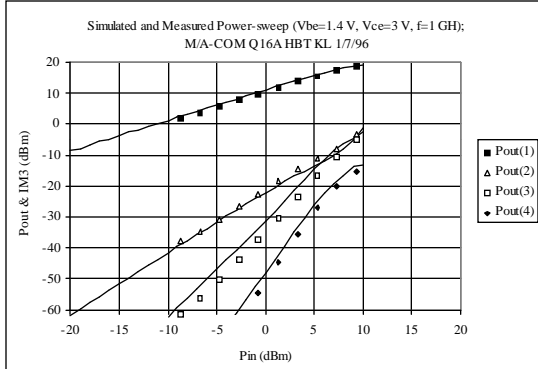


Fig.5 Measured and simulated power-sweep results under constant Vbe.

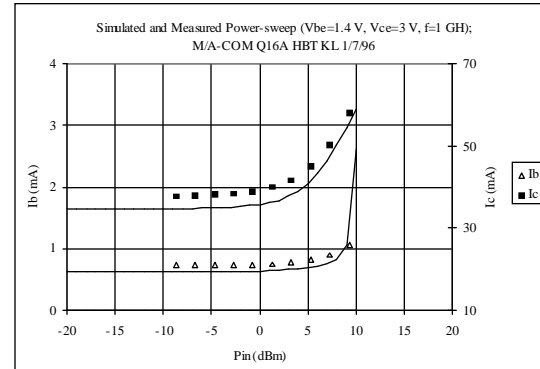


Fig.6 Measured and simulated bias point shift under constant Vbe.

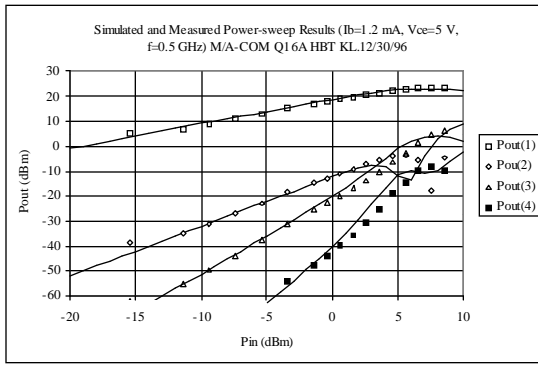


Fig.7 Measured and simulated power-sweep results under constant Ib.

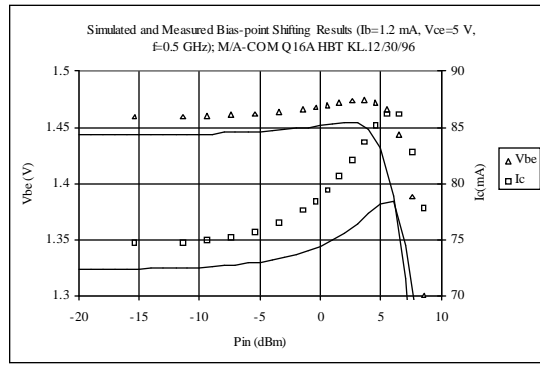


Fig.8 Measured and simulated bias point shift under constant Ib.

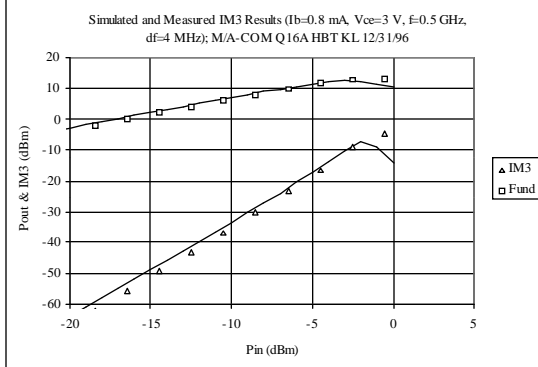


Fig.9 Measured and simulated IM3 results at 1 GHz.

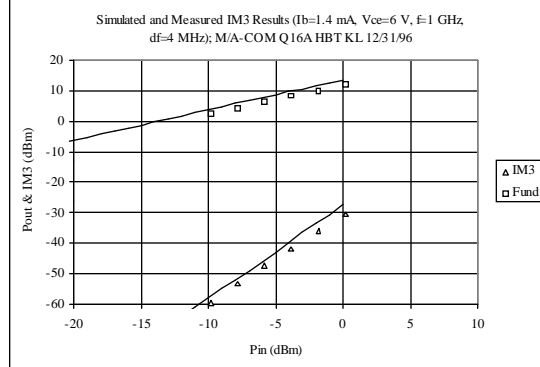


Fig.10 Measured and simulated IM3 results at 1 GHz.